Article

Optical Characterization of an Intra-Arterial Light and Drug Delivery System for Photodynamic Therapy of Atherosclerotic Plaque

Matthieu Zellweger [1] , **Ying Xiao** [1], **Manish Jain** [2] , **Marie-Noëlle Giraud** [2],
Andreas Pitzschke [1] , **Matthieu de Kalbermatten** [3], **Erwin Berger** [3], **Hubert van den Bergh** [4],
Stéphane Cook [2] **and Georges Wagnières** [1,*]

[1] LIFMET-IPHYS, Swiss Federal Institute of Technology (EPFL), 1015 Lausanne, Switzerland; Mpezellweger@yahoo.com (M.Z.); ying.xiao@epfl.ch (Y.X.); Andreas.Pitzschke@chuv.ch (A.P.)

[2] Cardiology, Department of Endocrinology, Metabolism and Cardiovascular System, Faculty of Science and Medicine, University and Hospital of Fribourg, 1708 Fribourg, Switzerland; manish.jain@unifr.ch (M.J.); Marie-noelle.giraud@unifr.ch (M.-N.G.); Stephane.cook@unifr.ch (S.C.)

[3] Acrostak AG, 8409 Winterthur, Switzerland; Mdekalb@yahoo.com (M.d.K.); info@acrostak.com (E.B.)

[4] LCOM-ISIC, Swiss Federal Institute of Technology (EPFL), 1015 Lausanne, Switzerland; Hubert.vandenbergh@epfl.ch

* Correspondence: Georges.wagnieres@epfl.ch

check for updates

Abstract: Although the versatility of photodynamic therapy (PDT) is well established, the technical aspects of light delivery systems vary significantly depending on the targeted organ. This article describes the optical properties of a light and drug delivery system (catheter and light diffuser) suitable for intra-arterial PDT by using a planar imaging goniometer to measure the full radiance longitudinal and angular profiles at the surface of the diffuser at 652 nm. The results show that the system emits almost Lambertian and "top hat" profiles, an interesting feature to determine the light dosimetry in the many vascular applications of PDT.

Keywords: light distributor radiometry; intra-arterial; photodynamic therapy; atherosclerosis

1. Introduction

The versatility of photodynamic therapy (PDT) as a treatment method for different diseases in various organs is well established. However, apart from the general principles underpinning the method, which are unchanged from organ to organ, the technical aspects of the treatment can vary greatly (including, but not limited to, choice of photosensitizer (PS), light dose and fluence rate, drug-light interval (DLI), PS dose and administration mode, and excitation wavelength). One such aspect pertains to light delivery, which is crucially impacted by the geometry, access and sterility properties of the target location. This aspect is particularly central for vascular PDT applications.

In organs with difficult geometries, care must be taken to use or develop suitable diffusers. This is the case for arterial applications of PDT, which have recently regained attention for plaque progression prevention [1–5]. Some studies have reported certain drawbacks (skin photosensitivity [6–8]; long DLIs [9,10]; heterogenous illumination leading to irregular effects [11], plaque stabilization instead of ablation or prevention of restenosis; use of PDT for vascular treatments limited to invasive procedures; limited use for acute events; long illumination times sometimes incompatible with clinical and physiological realities [12]), but local PS delivery and homogenous intra-arterial illumination often allow for circumventing them [2]. In all instances, the goal is to achieve a controlled and as

homogenous as possible fluence rate in the lesion without temperature increase in order to maximize the photodynamic effects whilst avoiding possibly deleterious side effects (thermal or otherwise) [13].

Although some studies positively describe external illuminations [14,15], pragmatism indicates that the best way to achieve suitable illumination of the coronaries is through endovascular light delivery, using a cylindrical (radial) diffuser such as the one described in Figure 1b or in [16–18].
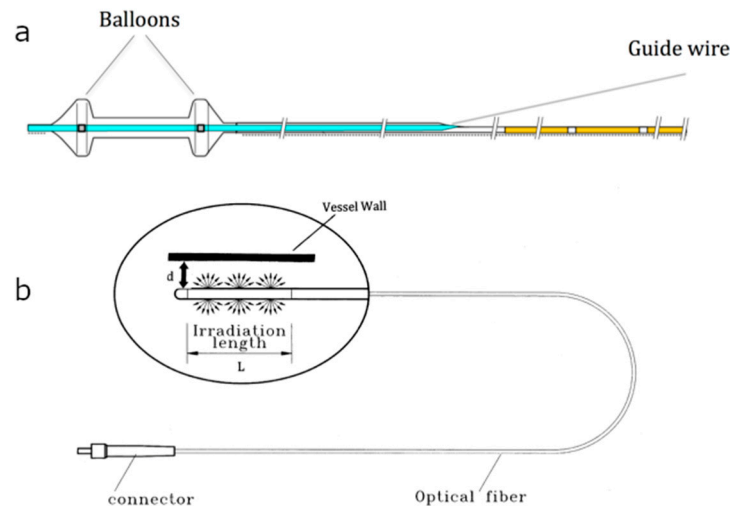

Figure 1. (**a**) Generic drawing of a stop-flow double balloon, multi-lumen nylon catheter (courtesy of Acrostak (Schweiz) AG); (**b**) generic drawing of a radial/cylindrical light diffuser for endovascular illumination (lower vessel wall omitted for clarity's sake, courtesy of Medlight SA, Ecublens, Switzerland).

As small (core diameters in the several hundreds of μm) optical fibers are usually used in these applications to deliver up to several hundreds of mW of light following an endovascular route, the natural choice is to use laser sources as light emitters [19]. The main advantage of laser sources for these applications is that they deliver relatively powerful and bright light beams, which can easily be coupled into optical fibers. It should be noted, however, that the nature of this coupling as well as the laser beam specifications have an important influence on the spatial and angular distributions of the intensity emitted by light distributors that are not equipped with mode scramblers.

Generally, radial/cylindrical diffusers offer an interesting way to deliver intravascular illumination for the treatment of acute coronary syndromes and regional atherosclerosis [5,20], especially for plaque stabilization, as opposed to plaque ablation [12].

In the specific case of diffusers used for the treatment of atherosclerotic plaque, numerous groups active in the field use fiber-based diffusers passed through catheters. Caution must be exercised in that case to ensure that the illumination profile of the 10–40 mm-long light-emitting windows is not modified by the catheter's material [21,22]. Longitudinal, azimuthal or radial uncontrolled variations of the light radiance by the catheter can lead to localized irregular light distribution and hence to undesirable effects due to local under- or over-treatments.

Similar caution must be exercised when the light distributor is centered within the vessel's lumen with an inflatable balloon. This approach is particularly appropriate when the fiber diameter is much smaller than the lumen diameter. Balloon catheters provide the benefit to interrupt blood flow to center the fiber in the vessel and to remove blood from the illuminated surface, features that are sometimes used intermittently [23,24]. Since it helps in minimizing blood presence in the treated areas, the absorption of the excitation light used for PDT is decreased [25]. Since the blood flow interruption is limited in duration, this feature of balloon catheters can be a disadvantage (limited total delivered light dose) or an advantage (limited risk of side effects) [26]. It should be noted that the duration of this interruption might be significantly increased using "perfusion catheters" that are designed so that the blood flow is not totally interrupted when the balloon is inflated.

Because they do not interrupt the blood flow, bare radial/cylindrical diffusers can be used for longer durations in small (<1 mm) vessels, but require that the illumination wavelength be chosen in the longer-wavelength part of the visible spectrum (>650 nm) to minimize light absorption by the blood. This also results in a comparatively deeper light penetration into tissues, and limits the possible side effects associated with intimal hyperplasia [13] or thrombosis [27]. Instances are reported [28] when the PDT effect described is too weak, a side effect that can be ascribed to the blood absorption of light [28–30].

In the case of a radial diffuser such as the one described in Figure 1b, it must distribute light with a longitudinal profile as close as possible to a top hat profile [31–33]. Consequently, the light dose (primary incidence) delivered at a given distance from the diffuser can be calculated relatively easily if the distance (d) between the diffuser surface and the vessel wall is smaller than the irradiation length (L) of the diffuser, d << L, see Figure 1b), in particular if its emission is Lambertian. It is noteworthy that, if d >> L, the parameter "d" affects not only the primary irradiance but also the shape of the illumination spot [16,33,34]. This second effect is particularly marked if the light emission (brightness) at the surface of the diffuser is not Lambertian (i.e., is backward- or forward-peaked), as described in detail and illustrated in [34]. This may result in a "translation" of the illumination spot relative to the light diffuser [11,34] with potentially dramatic consequences. Importantly, if the illumination is not Lambertian, light propagation in tissues becomes only isotropic at depths larger than $1/\mu_s'$ (where μ_s' is the reduced scattering coefficient). Thus, if the illumination is not Lambertian, the angular distribution of the radiance at the surface of the light distributor impacts the treatment of lesions thinner than 1 mm, since $\mu_s'^{-1}$ in the red part of the spectrum can reach several hundreds of microns [31,33,35]. This means that, for a Lambertian source, the decrease in fluence rate in tissues starts close to the vessel surface, whereas for a collimated source, this decrease starts up to 1 mm underneath this surface, i.e., when most photons have been scattered, thus impacting any possible PDT effect [34]. It should be noted that the angular distribution of the radiance at the surface of the light distributor also significantly impacts the fluence rate in deep-seated tissues.

Unfortunately, the frequent lack of detailed description of diffusers optical properties makes it somewhat difficult to directly compare different designs and to fully master the light dosimetry associated with a given instrumental configuration [31].

This report describes a system to achieve local, intra-arterial PS delivery (catheter) and illumination (diffuser). The light diffuser's optical properties are characterized, before and after introduction into a catheter, with a dedicated goniometer-based imaging setup designed to conveniently and rapidly measure the longitudinal, polar and azimuthal distributions of the radiance. The analysis of the images of the light emitted by cylindrical diffusers enables us to minimize the moving parts of this unique device and to avoid the bias frequently generated by fully goniometer-based setups.

2. Materials and Methods

2.1. Catheter and Diffuser

The catheter is a stop-flow double balloon, multi-lumen nylon catheter fitted with a guide wire (based on a modified version of the typical catheter presented in Figure 1a, courtesy of Acrostak AG, Winterthur, Switzerland, and reminiscent in its design and metrics of the GENIE™ commercial catheter supplied by Acrostak AG), allowing injection, filling of an artery segment with a photosensitizing solution and subsequent aspiration thereof. The treatment zone is 30 mm long, and the balloon diameter is 3.5 mm (radial dimension). This configuration allows the positioning of the balloons covering the zone to be treated, and manometer-controlled inflation of the balloons to temporarily interrupt the blood flow during the filling of the treatment zone.

The diffuser used in this study is a commercially available product for clinical investigation (Cylindrical Light Diffuser, model RD20/250) supplied by Medlight SA (Ecublens, Switzerland). Briefly, it is a thin and very flexible (minimum bending radius: 10 mm) cylindrical light diffuser made of a

plastic optical fiber with a radially emitting fiber tip producing (as per supplier documentation) a "radial light pattern, which is homogeneous all along the diffuser tip". The diffuser can be supplied with various light-emitting lengths (10, 20, 25, 30, 40, 50 and 70 mm). It was decided to use 20 mm, considering the typical size of the lesions to be treated. The core and overall diameter are 280 and 470 μm, respectively. The overall length of the diffuser, customized for our application, is 1 m from the SMA connector to the diffusing tip. The transmission is specified as 85% at 652 nm. The numerical aperture of the fiber is 0.48, and it is fitted with an SMA connecting plug. The diffuser specified maximum power density in air is 0.5 W/cm and its absolute maximum input power is 2.0 W (continuous wave in both cases).

2.2. Radiance Measurements

An imaging goniometer described in detail elsewhere [11] and presented in Figure 2 was used for the radiance measurements. In brief, this set-up uses a planar goniometer (arm length: 60 cm) to measure the angular and spatial values of the radiance at the surface of cylindrical light diffusers along two axes with a filtered scientific imaging camera (EM-CCD C9100-12, Hamamatsu, Hamamatsu City, Japan) fitted with a zoom lens (TV zoom lens H6 × 2.5R-MD3; 1:1.2, Fuji Photo Optical Co., LTD, Saitama City, Japan) and a neutral density filter of T = 0.1% to avoid saturation. The detector array has 512×512 pixels with pixel size of 16×16 μm^2. Images of the radiance were treated by image processing software developed in house to determine, at each angle θ, the longitudinal values of the radiance at the surface of the light diffuser [11]. Interestingly, this software also determines the value of the radiance for different azimuthal angles φ at the surface of the cylindrical light diffuser. Basically, the idea is to exploit the cylindrical symmetry of the diffuser to derive the radiance for different values of φ.
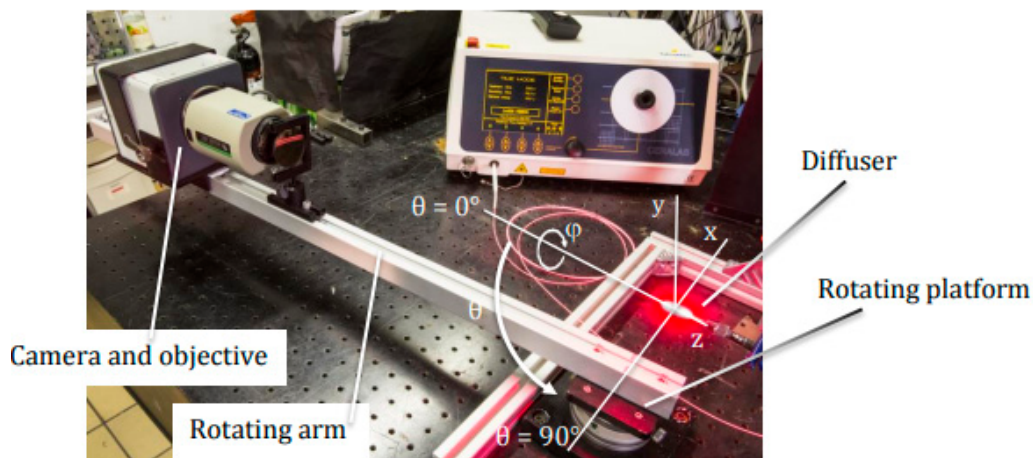

Figure 2. Goniometer setup: rotating platform, mechanical arm with EM-CDD camera, neutral density filter and diffuser holder. The polar angle θ (corresponding to the rotation of the camera around the vertical axis) and the azimuthal angle φ (obtained by measuring the radiance at different radial positions of the light diffusor image) are indicated. See [11] for a full description of the set-up.

The light diffuser, which integrates a mode scrambler, was connected to a 4 watt laser diode (Ceralas® PDT, 652 ± 4 nm/400 μm, CeramOptec GmbH, Bonn, Germany) and positioned parallel to the axis at the center of the goniometer's rotating platform, with or without the catheter external sheathing around it. Each resulting diagram shows the measurement of the radiance as a function of the longitudinal axis (Figure 3a), polar angle θ (Figure 3b,d, (*x*, *z*)-plane) or azimuthal angle φ (Figure 3c,e, *y*-axis). It is important to note that angles close to 0° and 180° (Figure 3b,c) were inaccessible to the line of sight of the camera due to the diffuser fixation blocking off the view. In a similar way, angles close to 90° and 270° (Figure 3c,e) were inaccessible to the line of sight of the camera due to emission being

parallel to the diffuser surface. Further details regarding this measurement setup and procedure are beyond the purpose of this paper and are described elsewhere [11].
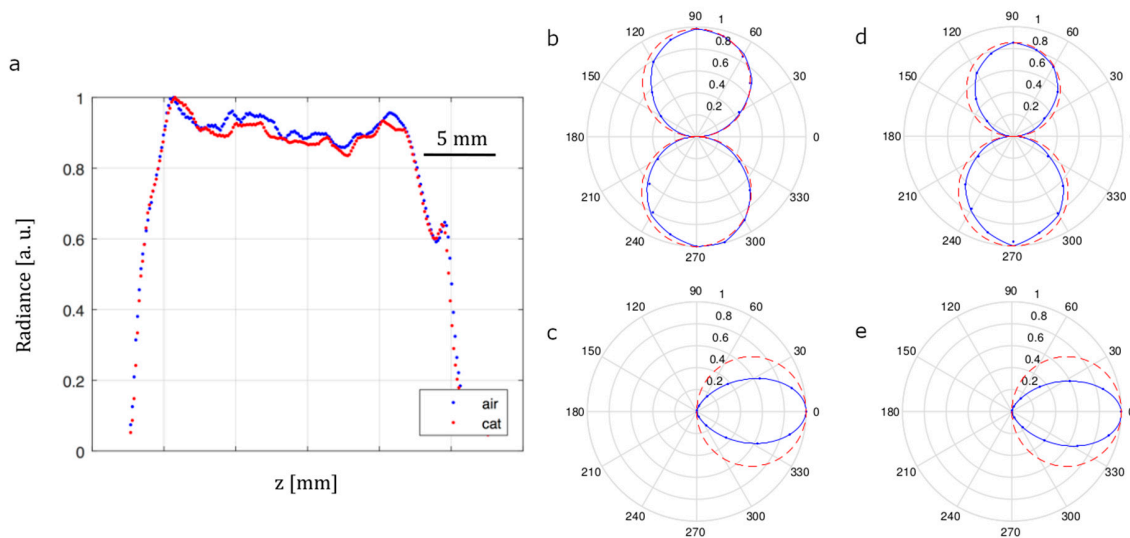

Figure 3. (**a**) Normalized longitudinal radiance profile of a radial/cylindrical light diffuser for endovascular illumination (at 652 nm in air (blue curve) or placed into a transparent vascular catheter sheathing (red curve, "cat"); = 0 deg.). The fiber distal end is located on the right. (**b**) Polar radiance profile of radial/cylindrical light diffuser for endovascular illumination (at 652 nm in air; φ = 0 deg.; arbitrary units). Red dotted line: Lambertian profile; blue line: measurements. Measurements and Lambertian profiles are superimposed at 90° and 270°. (**c**) Azimuthal radiance profile of radial/cylindrical light diffuser for endovascular illumination (at 652 nm in air; θ = 90 deg.; arbitrary units). Red dotted line: Lambertian profile; blue line: measurements. Measurements and Lambertian profiles are superimposed at φ = 0°. (**d**) Polar radiance profile of a radial/cylindrical light diffuser for endovascular illumination placed into a standard transparent vascular catheter (at 652 nm; φ = 0 deg.; arbitrary units) in air. Red dotted line: Lambertian profile; blue line: measurements. Measurements and Lambertian profiles are superimposed at 90° and 270°. (**e**) Azimuthal radiance profile of a radial/cylindrical light diffuser for endovascular illumination placed into a standard transparent vascular catheter (at 652 nm, θ = 90 deg.; arbitrary units) in air. Red dotted line: Lambertian profile; blue line: measurements. Measurements and Lambertian profiles are superimposed at φ = 0°.

3. Results

Typical profiles of a radial diffuser measured at 652 nm (with and without insertion in a catheter) are given in Figure 3.

The various profiles given in Figure 3 cover the measurements made to characterize the diffuser chosen for endovascular applications. Figure 3a shows the longitudinal radiance profile of a cylindrical light diffuser for endovascular illumination superimposed with the same measurement in the catheter sheathing material. Figure 3b shows the polar radiance profile of the same diffuser, in air, expressed as a function of the angle θ of the camera. It is fitted (for visual support only) with a theoretical Lambertian profile (red dotted line). Figure 3d shows the same measurement for the same diffuser placed into the catheter sheathing material. Figure 3c shows the azimuthal radiance profile of the same diffuser, in air, expressed as a function of the angle φ with the horizontal plane (*x*, *z*) where the camera rotates. It is fitted (for visual support only) with a theoretical Lambertian profile (red dotted line). Figure 3e shows the same measurement for the same diffuser placed into the catheter sheathing material. The intra-figure comparison of the two curves in Figure 3a and the pair comparison of Figure 3b,d, as well as Figure 3c,e indicate that, in all cases, the profile is only minimally modified by the insertion of the diffuser into the catheter sheathing.

4. Discussion

This study aimed at exploring concepts often overlooked in the context of PDT, in particular in intravascular PDT, namely the accurate and complete description of the light delivery to the target tissue by the light distributor.

The overall objective of the exploration was to fully characterize the angular distribution of the radiance at the surface of light distributors along two directions, in order to better master the desired therapeutic results. The radiance imaging setup used for this purpose is of great interest since, in spite of the concern potentially associated with a limited control of light distribution profile compared to what is expected, few light delivery systems are optically characterized in great detail [31,35,36]. This setup is original in the sense that it enables measuring the spatial and angular distribution of the radiance, which is a directional radiometric quantity, of cylindrical light distributors with a minimal number of moving parts. Indeed, the analysis of the images provided by this setup enables us to determine the value of the radiance according to one angle, the angle φ in the present study, in "real time" (potentially in a fraction of second), whereas fully goniometer-based setups are much less convenient and are more subject to bias [11]. Indeed, one critical problem faced by the conventional fully goniometer-based setups is in relation with their pointing stability while measuring the angular distribution of the radiance emitted by a "small" surface element of the distributor.

It should be noted that a cheap camera, optimized in terms of sensitivity, linearity and resolution for specific cylindrical light distributors, could be used to record the image, enabling us to determine the angular distribution of the radiance along one of the angles without moving parts.

The radiance measurements show that the diffuser emits a stable, almost ideal Lambertian profile at 652 nm, a wavelength of interest in PDT. Additional comparisons with its profiles at 635 (4 watts diode laser Ceralas® PDT, 635 ± 3 nm/400 µm, CeramOptec GmbH, Bonn, Germany) and 730 nm (Diode laser LTL730S 730 nm, TechLaser, Shanghai, China) showed that the diffusers' radiance profile was remarkably similar at these three wavelengths (data not shown). In addition, the profile is almost perfectly rectangular when measured longitudinally in air. This observation, combined with the almost perfectly Lambertian emission, is of importance to fully master the light dosimetry, and, as far as the longitudinal profile is concerned, is in good agreement with the claims of the manufacturer providing the cylindrical light distributor. This is also a positive result for possible clinical applications since it means that the diffuser can be aligned with the lesion to emit light where it is needed, with a minimal dependence on the vessel's diameter and on the chosen PS/illumination wavelength. The deviations from ideal longitudinal and Lambertian profiles probably have different origins. The longitudinal variations are likely to be due to a heterogeneous processing of the fiber core to decouple the light, whereas the deviations from a Lambertian profile are probably due to the Snell's law effect which takes place at the diffuser–air interface. Since the angular dispersion of the light exiting the diffuser is minimal for nearly orthogonal rays, this effect generates a forward-peaked emission, even if the light is isotropic in the distributor wall. It should be noted that this effect is probably significantly reduced if the distributor is surrounded by tissues or blood instead of air, since the refractive index step is reduced. The implications of these limited deviations on the treatment outcome are certainly minimal since the lengths of the longitudinal heterogeneities are smaller than the propagation length of red light in soft tissues [37]. Importantly, the deviations from ideal longitudinal profiles have a reduced effect if the distributor surface and the tissue are not in contact since the irradiance applied to the lesion results from the contribution of a large surface of the diffuser surface.

Wavelengths in the red or NIR are usually preferred to treat atherosclerotic plaque by PDT because of their deeper penetration in most soft tissues compared to shorter wavelengths [37]. In addition, their homogenous distribution in these tissues makes these wavelengths optimal for endovascular applications. Since their absorption is much smaller than their scattering in the blood vessel wall

or in the surrounding tissues, the fluence rate can be calculated using the diffusion approximation, as proposed by Ishimaru [38]. The steady-state expression to calculate the fluence rate in the tissue is:

$$(\Delta - \mu_{eff}^2)\phi(\mathbf{r}) = -q(\mathbf{r})/D, \tag{1}$$

where $\phi(\mathbf{r})$ is the fluence rate (mW/cm^2), $\mu_{eff} = [3\mu_a(\mu_a + \mu_s(1 - g)]^{1/2}$ is the effective attenuation coefficient (mm^{-1}), $D = \mu_a/\mu_{eff}^2$ is the optical diffusivity (mm), and q is the diffusive photon density (mW/cm^3). The absorption and scattering coefficients, μ_a (mm^{-1}) and μ_s (mm^{-1}), correspond to the inverse of the photon's mean free path before they are absorbed or scattered, respectively. g is the scattering anisotropy factor, which relates the reduced scattering μ_s' (mm^{-1}) and the scattering coefficients in the expression: $\mu_s' = \mu_s(1 - g)$.

The solution of Equation (1) for the fluence rate "far" (i.e., at several times $\mu_s'^{-1}$) from the source and interfaces produced by an infinitely long light diffuser inserted in a tissue in a cylindrically symmetric configuration is given by [39]:

$$\phi(r) = [(P/2\pi a)/(D\mu_{eff}K_1(\mu_{eff}\, a))]\, K_0(\mu_{eff}\, r), \tag{2}$$

where P is the optical power per unit length (mW/mm) of the light diffuser with radius a (mm). K_0 and K_1 are the modified Bessel K functions of the zero and first order, respectively. The distance from the diffuser axis is expressed as r (mm).

Since the length of light diffusers used to treat atherosclerotic plaque by PDT in coronary arteries ranges between 10 and 40 mm, and since their diameter is much smaller (between several hundreds of microns and one millimeter), expression (2) can be used if the diffuser is in contact with the vessel wall.

This expression can also be used if the light diffuser is inserted at the center of a transparent balloon, provided that the radius of this balloon is much smaller than μ_{eff}^{-1} and the length of the illuminated section of the artery. In that rare situation, which prevails only when NIR light is emitted by a small (diameter of 1 mm or less) balloon, the parameter a (mm) corresponds to its radius. This means that expression (2) can be used to calculate the fluence rate in the wall and around coronary arteries assuming uniform optical coefficients.

The picture is different if PDT is performed in larger vessels, as is the case for peripheral atherosclerotic disease. In that case, expression (2) is no longer valid since the radius of the vessel can be in the order of the diffuser's length. An estimate of the fluence rate in the tissues at depths "z" larger than 1 mm is given by expression (3) if the balloon radius and the diffuser's length are much larger than μ_{eff}^{-1} [40,41]. This situation is analogous to a "broad" (i.e., the two dimensions of the illumination spot are much larger than μ_{eff}^{-1}) uniform illumination of a "flat" (i.e., the smaller radius of curvature of the tissue surface is much larger than μ_{eff}^{-1}) air–tissue interface.

$$\phi(\mathbf{z}) = Ek\exp(-\mu_{eff}z), \tag{3}$$

where E is the irradiance (mW/cm^2), z (mm) is the distance from the air-tissue interface and k is a term that describes how backscattered light increases the irradiance delivered to the surface, yielding an elevated fluence rate near the surface. Its value, which is typically in the range of 3–6 for soft tissues in the red or NIR, depends on the tissue optical properties as well as on the refractive index matching conditions [41]. Its accurate value can be determined using Monte-Carlo simulations of the propagation of light [34,42,43]. In this case, however, the angular distribution of the radiance at the surface of the light distributor must be known, a situation illustrating the interest of performing directional radiometric measurements, as reported in this paper. Using optical coefficients compiled by Roggan [44] for the aorta at 630 nm, the value of k is about 5 if the refractive indexes are mismatched [41,43].

It should be noted that expressions (2) and (3) are solutions of the diffusion approximation. Therefore, these solutions are only valid if the hypotheses that are at the origin of this approximation are fulfilled, in particular if the light flux in the tissues is isotropic. This condition is clearly satisfied at

a much closer distance (less than $\mu_s'^{-1}$) from the light distributor if its emission is Lambertian rather than collimated, a fact that also illustrates the interest of multi-directional radiometric measurements. This concept is illustrated in Figure 4, which presents a comparison between the values of the normalized fluence rate determined according to Equation (3) or by Monte-Carlo simulations in the cases of broad illuminations of an air–tissue interface. This figure presents the evolution of the fluence with depth when the semi-infinite tissue, presenting the optical properties reported by Roggan [44] at 630 nm for the aorta, is subject to a collimated or a Lambertian illumination. The fluence rate is normalized in the sense that its absolute value is divided by the irradiance applied at the air–tissue interface. The Monte-Carlo simulation was based on commercially available software (Tracepro; Lambda Research Corporation, Littletown, MA, USA) and hardware described in details by Pitzschke et al. [45].
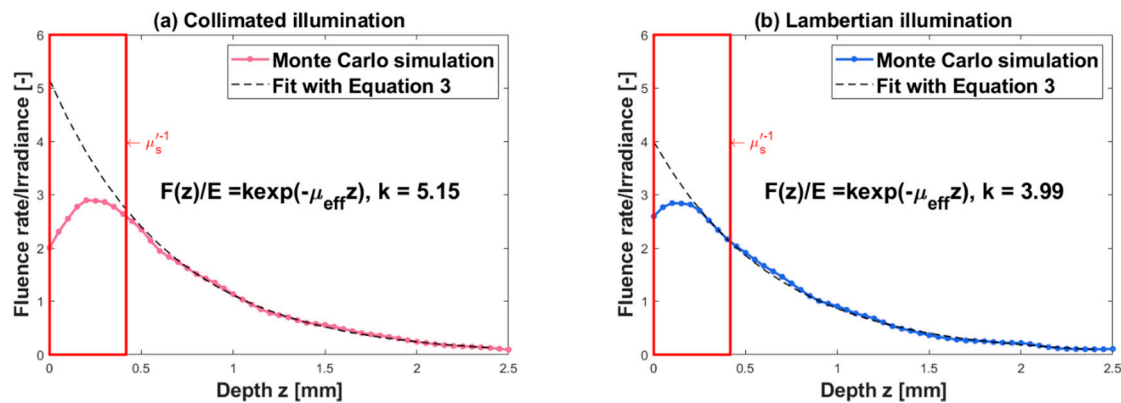

Figure 4. (**a**) Monte-Carlo simulation of the evolution of the normalized fluence with depth in a semi-infinite tissue presenting the optical properties reported by Roggan [44] at 630 nm for the aorta (μ_a = 0.29 mm^{-1}; μ_s' = 2.40 mm^{-1}; μ_{eff} = 1.53 mm^{-1}). The air–tissue interface is illuminated at 90 degrees with a broad and collimated light beam. The dashed line corresponds to a fit of the simulation with Equation (3). (**b**) Same condition, excepting that the illumination of the air–tissue interface is Lambertian.

As illustrated in Figure 4, the shape of the fluence rate is significantly different, for an identical irradiance, at the tissue "surface" (where atherosclerotic plaques potentially sit) if the illumination is collimated or Lambertian. This difference is significant down to about 0.4 mm, i.e., $\mu_s'^{-1}$, as expected (see the red squares). Importantly, the pre-exponential factor "k", used to fit the spatial evolution of the fluence rate with a solution of the diffusion approximation (Equation (3)), decreases from about 5.15 to 3.99 (more than 25% difference in our conditions) when a Lambertian illumination is considered instead of a collimated one. As a consequence, the nature of the tissue illumination (collimated or Lambertian) affects the fluence rate significantly, even in deep-seated tissues.

If, depending on the light delivery design, the balloon or the diffuser radius is comparable to μ_{eff}^{-1}, as is the case when red light is used to treat plaque in the carotid, neither expression (2) nor (3) is valid. It should be noted, however, that the fluence rate can still be estimated analytically since it is confined within an interval defined by the values calculated with these two expressions, as discussed by Profio et al. [40].

When calculating the light dosimetry for the treatment of atherosclerotic plaque by PDT, it is important to consider edge effects. These effects are significant, in particular if the diffuser length is in the order of μ_{eff}^{-1}. They are due to the lateral spreading of light within the tissues. This spreading is balanced and canceled at the center of the illuminated area, whereas it is not the case close to the edges where lateral diffusion is unbalanced. As described by Jacques [41], edge losses at the periphery of a longitudinally uniform beam extend about $3\mu_{eff}^{-1}$ from the beam edge. This corresponds to about 4 mm when using the optical coefficients reported by Roggan [37,44] at 630 nm for the aorta.

Only when the extent of the illuminated area exceeds $6\mu_{\text{eff}}^{-1}$ is the fluence rate in the central zone (where the plaque is supposed to be located) longitudinally uniform.

Finally, it should be noted that the plaque itself frequently presents optical properties that are not only heterogeneous but also significantly different compared to those of the normal surrounding tissues [46]. Since these optical properties cannot realistically be determined before each treatment, one reasonable strategy is to adjust the light dosimetry on the basis of the type of plaque to be treated.

Intra-arterial applications require that the diffuser be inserted into a catheter to reach the desired position. The measurements reported here for a modified commercially available catheter designed for drug delivery demonstrated that the plastic sheathing produced by this specific catheter has virtually no impact on the light emission profile of the diffuser, making it a suitable system to illuminate optimally intra-arterial lesions and avoid absorption, with a possible resulting heating, or a patchy or irregular illumination pattern, which could possibly have negative consequences.

Overall, these results show that this system displays optimal illumination and dosimetry properties to achieve the sought-after results.

Author Contributions: Conceptualization, M.Z., M.-N.G., A.P., E.B., S.C. and G.W.; Data curation, M.Z., Y.X., A.P. and G.W.; Formal analysis, M.Z., Y.X., A.P. and G.W.; Project administration, M.-N.G., S.C. and G.W.; Resources, A.P., Y.X., M.d.K., E.B., H.v.d.B. and G.W.; Validation, M.Z., Y.X., M.J., M.-N.G., A.P., M.d.K., E.B., H.v.d.B., S.C. and G.W.; Writing—original draft, M.Z., A.P. and G.W.; Writing—review & editing, M.Z., A.P. and G.W. All authors have read and agreed to the published version of the manuscript.

Conflicts of Interest: G.W. is a shareholder of Medlight SA. M.d.K. and E.B. were employed by Acrostak SA at the time of this study. The other authors have no relevant financial interests in this article and no potential conflicts of interest to disclose.

References

1. Hamada, R.; Matsuzaki, R.; Ogawa, E.; Arai, T. Patency of heart blood vessels under photosensitization reaction shortly after intravenous injection of talaporfin sodium in canine model. In Proceedings of the Optical Interactions with Tissue and Cells XXVII, San Francisco, CA, USA, 7 March 2016; p. 9706.

2. Jain, M.; Zellweger, M.; Frobert, A.; Valentin, J.; van den Bergh, H.; Wagnières, G.; Cook, S.; Giraud, M.-N. Intra-Arterial Drug and Light Delivery for Photodynamic Therapy Using Visudyne®: Implication for Atherosclerotic Plaque Treatment. *Front. Physiol.* **2016**, *7*, 400. [CrossRef]

3. Peng, C.; Li, Y.; Liang, H.; Cheng, J.; Li, Q.; Sun, X.; Li, Z.; Wang, F.; Guo, Y.; Tian, Z.; et al. Detection and photodynamic therapy of inflamed atherosclerotic plaques in the carotid artery of rabbits. *J. Photochem. Photobiol. B Boil.* **2011**, *102*, 26–31. [CrossRef] [PubMed]

4. Maslaňáková, M.; Balogová, L.; Miškovský, P.; Tkáčová, R.; Stroffekova, K. Anti- and Pro-apoptotic Bcl2 Proteins Distribution and Metabolic Profile in Human Coronary Aorta Endothelial Cells before and after HypPDT. *Cell Biophys.* **2016**, *74*, 435–447. [CrossRef] [PubMed]

5. Waksman, R.; Leitch, I.M.; Roessler, J.; Yazdi, H.; Seabron, R.; Tio, F.; Scott, R.W.; Grove, R.I.; Rychnovsky, S.; Robinson, B.; et al. Intracoronary photodynamic therapy reduces neointimal growth without suppressing re-endothelialisation in a porcine model. *Heart* **2006**, *92*, 1138–1144. [CrossRef] [PubMed]

6. Wooten, R.S.; Smith, K.C.; Ahlquist, D.A.; Muller, S.A.; Balm, R.K. Prospective study of cutaneous phototoxicity after systemic hematoporphyrin derivative. *Lasers Surg. Med.* **1988**, *8*, 294–300. [CrossRef]

7. Dougherty, T.J.; Cooper, M.T.; Mang, T.S. Cutaneous phototoxic occurrences in patients receiving Photofrin®. *Lasers Surg. Med.* **1990**, *10*, 485–488. [CrossRef]

8. Wagnieres, G.; Hadjur, C.; Grosjean, P.; Braichotte, D.; Savary, J.F.; Monnier, P.; van den Bergh, H. Clinical evaluation of the cutaneous phototoxicity of 5,10,15,20-tetra(m-hydroxyphenyl)chlorin. *Photochem. Photobiol.* **1998**, *68*, 382–387. [CrossRef]

9. Kereiakes, D.J.; Szyniszewski, A.M.; Wahr, D.; Herrmann, H.C.; Simon, D.I.; Rogers, C.; Kramer, P.; Shear, W.; Yeung, A.C.; Shunk, K.A.; et al. Phase I drug and light dose-escalation trial of motexafin lutetium and far red light activation (phototherapy) in subjects with coronary artery disease undergoing percutaneous coronary intervention and stent deployment: Procedural and long-term results. *Circulation* **2003**, *108*, 1310–1315. [CrossRef]

10. Tawakol, A.; Castano, A.P.; Anatelli, F.; Bashian, G.; Stern, J.; Zahra, T.; Gad, F.; Chirico, S.; Ahmadi, A.; Fischman, A.J.; et al. Photosensitizer delivery to vulnerable atherosclerotic plaque: Comparison of macrophage-targeted conjugate versus free chlorin(e6). *J. Biomed. Opt.* **2006**, *11*, 021008. [CrossRef]

11. Pitzschke, A.; Bertholet, J.; Lovisa, B.; Zellweger, M.; Wagnières, G. Determination of the radiance of cylindrical light diffusers: Design of a one-axis charge-coupled device camera-based goniometer setup. *J. Biomed. Opt.* **2017**, *22*, 1–9. [CrossRef]

12. Muller, J.E. New Light on an Old Problem, Photodynamic Therapy for Atherosclerosis. *J. Am. Coll. Cardiol.* **2008**, *52*, 1033–1034. [CrossRef] [PubMed]

13. Borshch, V.N.; Andreeva, E.R.; Kuzmin, S.G.; Vozovikov, I.N. New medicines and approaches to treatment of atherosclerosis. *Russ. J. Gen. Chem.* **2012**, *82*, 554–563. [CrossRef]

14. Wakamatsu, T.; Saito, T.; Hayashi, J.; Takeichi, T.; Kitamoto, K.; Aizawa, K. Long-term inhibition of intimal hyperplasia using vascular photodynamic therapy in balloon-injured carotid arteries. *Med. Mol. Morphol.* **2005**, *38*, 225–232. [CrossRef] [PubMed]

15. Spears, J.R. Percutaneous laser treatment of atherosclerosis: An overview of emerging techniques. *Cardiovasc. Interv. Radiol.* **1986**, *9*, 303–312. [CrossRef] [PubMed]

16. Lilge, L.; Vesselov, L.; Whittington, W. Thin Cylindrical Diffusers in Multimode Ge-Doped Silica Fibers. *Lasers Surg. Med.* **2005**, *36*, 245–251. [CrossRef] [PubMed]

17. Charles Lytle, A.; Narciso, H.L.; Spain, D.V.; Doiron, D.R. Third generation cylindrical diffusers for medical use. In Proceedings of the SPIE Optical Fibers in Medicine VIII, Los Angeles, CA, USA, 21 January 1993; pp. 195–201.

18. Mizeret, J.; van den Bergh, H. Cylindrical Fiberoptic Light Diffuser for Medical Applications. *Lasers Surg. Med.* **1996**, *19*, 159–167. [CrossRef]

19. Chou, T.M.; Woodburn, K.W.; Cheong, W.-F.; Lacy, S.A.; Sudhir, K.; Adelman, D.C.; Wahr, D. Photodynamic Therapy: Applications in atherosclerotic vascular disease with Motexafin Lutetium, catheterization and cardiovascular interventions. *Cathet. Cardiovasc. Interv.* **2002**, *57*, 387–394. [CrossRef]

20. Waksman, R.; McEwan, P.E.; Moore, T.; Pakala, R.; Kolodgie, F.D.; Hellinga, D.G.; Seabron, R.C.; Rychnovsky, S.J.; Vasek, J.; Scott, R.W.; et al. PhotoPoint Photodynamic Therapy Promotes Stabilization of Atherosclerotic Plaques and Inhibits Plaque Progression. *J. Am. Coll. Cardiol.* **2008**, *52*, 1024–1032. [CrossRef]

21. Dwyer, P.J.; White, W.M.; Fabian, R.L.; Anderson, R.R. Optical integrating balloon device for photodynamic therapy. *Lasers Surg. Med.* **2000**, *26*, 58–66. [CrossRef]

22. Van den Bergh, H. On the evolution of some endoscopic light delivery systems for photodynamic therapy. *Endoscopy* **1998**, *30*, 392–407. [CrossRef]

23. Jenkins, M.P.; Buonaccorsi, G.A.; Mansfield, R.; Bishop, C.C.; Bown, S.G.; McEwan, J.R. Reduction in the response to coronary and iliac artery injury with photodynamic therapy using 5-aminolaevulinic acid. *Cardiovasc. Res.* **2000**, *45*, 478–485. [CrossRef]

24. Jenkins, M.P.; Buonaccorsi, G.A.; Raphael, M.; Nyamekye, I.; McEwan, J.R.; Bown, S.G.; Bishop, C.C.R. Clinical study of adjuvant photodynamic therapy to reduce restenosis following femoral angioplasty. *BJS* **1999**, *86*, 1258–1263. [CrossRef] [PubMed]

25. Vincent, G.M.; Fox, J.; Charlton, G.; Hill, J.S.; McClane, R.; Spikes, J.D. Presence of blood significantly decreases transmission of 630 nm laser light. *Lasers Surg. Med.* **1991**, *11*, 399–403. [CrossRef] [PubMed]

26. Mansfield, R.; Bown, S.; McEwan, J. Photodynamic therapy: Shedding light on restenosis. *Heart* **2001**, *86*, 612–618. [CrossRef]

27. Kossodo, S.; LaMuraglia, G.M. Clinical potential of photodynamic therapy in cardiovascular disorders. *Am. J. Cardiovasc. Drugs* **2001**, *1*, 15–21. [CrossRef]

28. Rockson, S.G.; Lorenz, D.P.; Cheong, W.F.; Woodburn, K.W. Photoangioplasty: An emerging clinical cardiovascular role for photodynamic therapy. *Circulation* **2000**, *102*, 591–596. [CrossRef]

29. Vincent, G.M.; Mackie, R.W.; Orme, E.; Fox, J.; Johnson, M. In Vivo Photosensitizer-Enhanced Laser Angioplasty in Atherosclerotic Yucatan Miniswine. *J. Clin. Laser Med. Surg.* **1990**, *8*, 59–61. [CrossRef]

30. Litvack, F.; Grundfest, W.S.; Forrester, J.S.; Fishbein, M.C.; Swan, H.; Corday, E.; Rider, D.M.; McDermid, I.S.; Pacala, T.J.; Laudenslager, J.B. Effect of hematoporphyrin derivative and photodynamic therapy on atherosclerotic rabbits. *Am. J. Cardiol.* **1985**, *56*, 667–671. [CrossRef]

31. Ripley, P.; Mills, T.; Brookes, J. Measurement of the Emission Profiles of Cylindrical Light Diffusers Using a Video Technique. *Lasers Med Sci.* **1999**, *14*, 67–72. [CrossRef]

32. Small, W.; Buckley, P.R.; Wilson, T.S.; Loge, J.M.; Maitland, K.; Maitland, D.J. Fabrication and characterization of cylindrical light diffusers comprised of shape memory polymer. *J. Biomed. Opt.* **2008**, *13*, 024018. [CrossRef]

33. Vesselov, L.M.; Whittington, W.; Lilge, L. Performance evaluation of cylindrical fiber optic light diffusers for biomedical applications. *Lasers Surg. Med.* **2004**, *34*, 348–351. [CrossRef] [PubMed]

34. Farina, B.; Saponaro, S.; Pignoli, E.; Tomatis, S.; Marchesini, R. Monte Carlo simulation of light fluence in tissue in a cylindrical diffusing fibre geometry. *Phys. Med. Boil.* **1999**, *44*, 1–11. [CrossRef] [PubMed]

35. Murrer, L.H.P.; Marijnissen, J.P.A.; Star, W.M. Light distribution by linear diffusing sources for photodynamic therapy. *Phys. Med. Boil.* **1996**, *41*, 951–961. [CrossRef] [PubMed]

36. Guo, Z.; Daly, S.R.; Matson, J.K. Optical modeling of cylindrical light sources within tissue. *Proc. SPIE* **2003**, *4961*, 114.

37. Roggan, A.; Friebel, M.; Dörschel, K.; Hahn, A.; Müller, G. Optical Properties of Circulating Human Blood in the Wavelength Range 400–2500 nm. *J. Biomed. Opt.* **1999**, *4*, 36–46. [CrossRef]

38. Ishimaru, A. *Wave Propagation and Scattering in Random Media*; Academic Press: New York, NY, USA, 1978.

39. Tromberg, B.J.; Svaasand, L.O.; Fehr, M.K.; Madsen, S.J.; Wyss, P.; Sansone, B.; Tadir, Y. A mathematical model for light dosimetry in photodynamic destruction of human endometrium. *Phys. Med. Boil.* **1996**, *41*, 223–237. [CrossRef]

40. Profio, A.E.; Doiron, D.R. Transport of light in tissue in photodynamic therapy. *Photochem. Photobiol.* **1987**, *46*, 591–599. [CrossRef]

41. Jacques, S.L. How tissue optics affect dosimetry of photodynamic therapy. *J. Biomed. Opt.* **2010**, *15*, 051608. [CrossRef]

42. Wang, L.-H.; Jacques, S.L.; Zheng, L.-Q. MCML–Monte Carlo modeling of photon transport in multi-layered tissues. *Comput. Methods Programs Biomed.* **1995**, *47*, 131–146. [CrossRef]

43. Flock, S.; Wilson, B.C.; Patterson, M.S. Monte Carlo modeling of light propagation in highly scattering tissues, I: Model predictions and comparison with diffusion theory, II Comparison measurements in phantoms. *IEEE Trans. Biomed. Eng.* **1989**, *36*, 1162–1173. [CrossRef]

44. Roggan, A. *Dosimetrie thermischer Laseranwendungen in der Medizin*; Ecomed: West Auckland, New Zealand, 1997.

45. Pitzschke, A.; Lovisa, B.; Seydoux, O.; Zellweger, M.; Pfleiderer, M.; Tardy, Y.; Wagnieres, G. Red and NIR light dosimetry in the human deep brain. *Phys. Med. Biol.* **2015**, *60*, 2921–2937. [CrossRef] [PubMed]

46. Prince, M.R.; Deutsch, T.F.; Mathews-Roth, M.M.; Margolis, R.; Parrish, J.A.; Oseroff, A.R. Preferential light absorption in atheromas in vitro: Implications for laser angioplasty. *J. Clin. Investig.* **1986**, *78*, 295–302. [CrossRef] [PubMed]